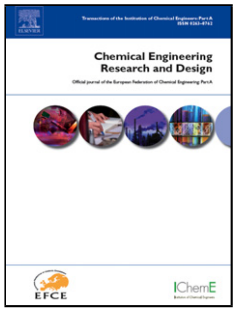

Title: Computation of steady state thermochemistry in rotary kilns: application to the cement clinker manufacturing process

Author: Vincent Meyer Alexander Pisch Karri Penttilä Pertti Koukkari

PII: S0263-8762(16)30223-4
DOI: http://dx.doi.org/doi:10.1016/j.cherd.2016.08.007
Reference: CHERD 2358

To appear in:

Received date: 31-3-2016
Revised date: 28-7-2016
Accepted date: 4-8-2016

Please cite this article as: Meyer, V., Pisch, A., Penttilä, K., Koukkari, P.,Computation of steady state thermochemistry in rotary kilns: application to the cement clinker manufacturing process, *Chemical Engineering Research and Design* (2016), http://dx.doi.org/10.1016/j.cherd.2016.08.007

Computation of steady state thermochemistry in rotary kilns: application to the cement clinker manufacturing process

Vincent Meyer[1], Alexander Pisch[1]

Karri Penttilä[2], Pertti Koukkari[2]

[1]*LafargeHolcim R&D, 95 rue du Montmurier – BP15, 38291 St Quentin-Fallavier, France*
firstname.lastname@lafargeholcim.com

[2]*VTT, P.O. Box 1401, FIN 02041-VTT, Finland*
firstname.lastname@vtt.fi

Abstract

Advanced Gibbs Free energy minimization was applied for modeling physical and chemical processes in various industrial rotary kilns. The method is the core of a generic computer program (KilnSimu), used to simulate kiln operations with different multiphase chemistries. KilnSimu combines iterative solution of the balance equations coupled with the Gibbs energy calculation of the kiln thermochemistry, thus providing a detailed quantitative analysis of the chemical and phase transformations as well as of mass and heat flows inside the kiln. Adding reaction rate constraints into the Gibbs energy procedure allows for the necessary reaction kinetics in the simulation. The calculation results are typically given as 1-dimensional steady state axial profiles in the longitudinal direction of the kiln.

The presented model was applied to an industrial problem in cement clinker manufacturing. The impact of pure oxygen addition at the main burner on the specific heat consumption of the full process was evaluated.

Keywords: rotary kiln**,** simulation, Gibbs energy minimization, reaction rate constraint, steady state, cement clinkering,

Computation of steady state thermochemistry in rotary kilns: application to the cement clinker manufacturing process

1. Introduction

The technology of rotating drums for heating, drying and calcining has been available for over 100 years. Industrial rotary kilns are used for purposes ranging from drying to combustible incineration and mineral and metallurgical processing. The kiln typically consists of a revolving cylindrical shell slightly inclined toward the outlet. The length of the shell varies from 10 to 100 meters, while the diameter may exceed 4 m. Wet, or pre-heated and dried feed of solids enters one end of the kiln and the dry material discharges from the other. Rotary kilns are usually heated by direct contact of hot gas flowing in opposite direction with the bed (Figure 1). The fuel is fed to a burner located at the end of the kiln, sometimes positioned in a separate chamber. The tilted, rotating drum then has the condensed material in slow movement in the axial direction, normally against the hot gas flow in the freeboard. Excluding the mild condition dryer and granulator applications, the common feature of the kiln operations is the complex chemistry which takes place in the different regions of both the bed and freeboard. A rotary kiln is therefore fundamentally a reactive heat exchanger where energy from a hot gas phase is transferred to the condensed bed material. The most well-known uses of rotary kilns are in pigment and lime calcination, in manufacturing cement clinker and calcination of alumina hydrates. Other bulky uses appear in the calcining of petroleum coke and in metallurgy, including roasting or reduction of ores, recycling of zinc and lead as oxides etc. Incineration of waste materials into non-toxic solids or recycling their contents (e.g.zinc, phosphorus) as re-usable products is a recent application, gaining constantly more ground. The wide choice of usages is due to the

flexibility in handling different kinds of feedstock from slumped and granular solids to wet slurries. In many cases, the ability of the rotary kiln to process the material into a desired grain size or particulate form is also beneficial, as well as the ability to maintain different redox conditions for the freeboard and for the condensed bed (Boateng 2008).

The kilns for various applications appear in several forms and shapes, with a wide range of geometries, structural and refractory (wall) materials depending on the operating conditions. They may be equipped with dams to increase the residence time of the material, with chains to remove sticky portions from the wall as well as with lifters or tumblers to improve the axial movement and mixing. All such features will affect the pursuit to simulate the transport phenomena occurring particularly in the bed phase.

The flame temperatures in rotary kilns may exceed 2000 K, and the processes occurring are due to the heat exchange from the hot gas phase to the bed material. The bed will then undergo changes due to its absorption of heat, a conventional sequence being drying with subsequent heating, followed by calcining or more complex chemical reactions.

High temperature processes occurring in kilns are major consumers of energy as well as producers of CO_2 emissions. Both the raw material and fuel often appear as CO_2-sources and historically the burner designs are for fossil fuels such as powdered coke and heavy oil. A typical lime kiln, for example, produces 170 TPD (tonnes per day) of carbon dioxide from the powder coke fuel per its 100 TPD of CO_2 from the raw limestone ($CaCO_3$).

Contemporary industry has pertinent interest in reduction of such environmental impact and in improving resource and energy efficiency of processes. There is then also apparent incentive to optimize rotary kiln operations, as significant savings are attainable when changing operational practices (e.g. Mager & al. 2000). The key questions then become how to design the burner in order to maximize the fuel efficiency and heat transfer from the burner flame to the bed**,** how to control the secondary air and fuel inlets to minimize energy

consumption at desired output and finally whether the fossil fuel can be switched to biofuel without compromising the kiln operation and product quality. Raw materials as well as the fuels used as heat sources also vary in their chemical composition, which has led to increasing interest in the complex chemistry and internal processes of the rotary drums. Critical process information including internal temperature of the gas and bed streams and their chemical composition can often only be inferred through indirect measurements. To compensate the shortage of observations, improved computational methods have been developed for better understanding of the kiln operations.

2. Methods used in kiln modeling

Optimization of rotary kilns will benefit from appropriate simulation models, which include accurate description of the chemical and physical processes inside. The modelling of the counter-current reactor with several chemical reactions, in combination with heat and mass transfer in a heterogeneous (multi-phase) system has yet remained a somewhat incompletely solved problem. Mostly, the mathematical analysis is based on the heat and mass balance considerations for the countercurrent solid and gas streams, to which some of the specific chemical and phase changes were added using assumptions on their reaction kinetics (e.g. Manitius et al. 1974, Dumont and Belanger 1978, Barr et al. 1989, Boateng and Barr 1996, Marias et al. 2005, Mujumdar and Ranade 2006, Boateng 2008, Pisaroni &al. 2012). As for a recent work on model based predictive controls see e.g. Stadler et al. 2011. In such developments, however the detailed chemistry of the kiln is further omitted and merely a rough compartment segmentation of the kiln (based on the aforementioned early developments) is further applied. Thus, the simulation model inherently will consist of a rather large set of ordinary differential equations and algebraic formulas, with their necessary boundary values.

Mujumdar and Ranade (2006) divide the rotary kiln models into two groups. The first group is the conventional solution of 1-dimensional material and energy balances for both the condensed bed and gas flows. Such models have been presented e.g. by Manitius et al. (1974) for the aluminium oxide kiln and Dumont and Belanger (1978) for the titanium dioxide calciner. For cement kilns Boateng and Barr (1996) presented a 'quasi 3-dimensional' approach, in which a 2-dimensional presentation for the transverse surface of the bed has been used, while the gas freeboard is treated with a 1-dimensional model. As the second group one may distinguish the models where a one-dimensional treatise is used to simulate the reactions in the bed region and for the freeboard, either experimental data or a detailed three-dimensional CFD based model is applied (Mastrorakos & al 1996, Mujumdar and Ranade 2006).

For both groups of the traditional models it is typical that the chemistry of the kilns is presented in terms of selected stoichiometric reactions, for which either a mechanistic reaction rate or an equilibrium condition is defined. The model of Mujumdar & al. (2007) for the cement kiln appears to be one of the most advanced, with 6 independent reactions for the solid phase, salient reaction rates for the combustion reactions in the gas phase and with a semi-empirical correlation for the formation of melt in the furnace. The reactions in the solid bed involve six components, viz. $CaCO_3$, CaO, C_2S, C_3S, C_3A and C_4AF (Ca-silicates, Ca-aluminate and Ca-aluminate-ferrite in cement notation, see Table 5). However, in such a case a number of important components and even elements (such as magnesium, sulphur or chlorine) are omitted. The molten (slag) phase is not identified as part of the heterogeneous multiphase system although various empirical temperature-dependent correlations can be used to incorporate the formation of the melt phase e.g. in cement kilns (Mujumdar et al. 2007).

To improve the insight on the complex chemical reactions in the bed, it is also possible to use multiphase thermochemical approach to recognize the formation of various compounds and phases in rotary kilns. A thermodynamic model for the lime calciner used in the pulp and paper industries was proposed by Backman et al. (1993). Ginsberg et al. (2005) have carried out a simulation of a cement furnace by using a combined thermochemical equilibrium calculation and CFD based combustion and clinker formation model for the cement furnace. Marias & al. (2005) constructed a model for the physico-chemical processes occurring when particles of aluminium coated with organic materials are introduced into a rotary kiln in order to be cleared of their organic content. The gas phase was modelled with a combination of CFD and multicomponent Gibbs energy minimization. For the bed phase as well a number of models including Gibbs'ian thermodynamics have been published (see eg. Backman et al 1993, Barry and Glasser 2000, Modigell et al. 2002, Eriksson et al. 2014). The multiphase thermodynamic treatment allows for the analysis of the chemical behaviour of important minor elements such as Mg, Al, Zn, S, Cl and K in the furnace. Another advantage of the thermodynamic approach is its easy adaptation to different chemical systems.

Yet, the chemical and phase changes within the kiln seldom reach equilibrium but rather appear in local steady state conditions. With predefined or assumed temperature profiles in the calculation, the models based on successive thermochemical states lack the possibility to validate the model with independent measurement from various parts of the furnace. However, techniques to incorporate reaction rate constraints for the kinetically slow reactions within a multiphase thermodynamic program are available for quite some time (Koukkari 1993, 1995, Koukkari & al. 1997). Such approach allows for the analysis of the kiln chemistry and phase changes according to thermodynamic principles, while also includes the necessary constraining of slow reaction kinetics. First programmed for the calcination of TiO_2 –pigment the program was used for off-line simulation for the development of process

controls (Pettilä 1996, Ketonen &al. 1997). The generic approach that combines the dynamic thermochemical processes with heat and mass transfer in the stationary operating kilns has made it possible to use the same procedure to several industrial simulation problems, including lime calcination, cement making, zinc oxide recovery in Waelz-kilns, waste incineration and for various metallurgical problems (Yokota 2009, gtt.mch.rwth-aachen.de 2014, vttresearch.com 2015, rccm.co.jp 2015).

3. Theory

3.1 Problem set for the multiphase thermochemical kiln model

According to the early treatment of e.g. Manitius et al. (1974), the essential phenomena in the rotary furnace can be described by the following type of equations: (i) equations of reaction kinetics; (ii) mass balance equations; (iii) heat balance equations; (iv) variable parameter formulae. Equations (i)-(iii) are differential equations, while (iv) are formed from a set of algebraic expressions. The algebraic formulae of (iv) describe the geometry of the furnace, the properties of reactant mixtures such as heat capacities, emissivities, viscosities and the like as well as the properties of the wall materials of the kiln, thermal conductivity being then the most important factor. The solution of the differential equations (i)-(iii) requires initial values for the temperatures of the solid and gas streams to be used as boundary conditions. As well the initial values of the solid and gas flow rate (axial) must be assumed. Zhou and Boateng (2008) divide these balances into their more basic factors listing (1) the continuity equation for mass flow, (2) momentum equation, (3) concentration transport equation (4) enthalpy transport equation and finally (5) Arrhenius equation for chemical reaction kinetics and (6) equation of state for the gaseous stream. The received equations for these balances become strongly non-linear in temperature, their solution becoming increasingly elaborate when complex chemistry of the reacting substances are taken into account.

Calculation of the complex chemistry in the rotary kilns becomes somewhat more simple by using the multi-component thermodynamic technique; i.e. by presenting both the gas stream and the solids stream as a series of thermodynamic states. For a steady state solution then rate-dependent phenomena of both reaction kinetics and heat and mass transfer need to be combined with the calculation of the thermodynamic properties. A single algorithm is used to combine these factors for each control volume element in the furnace. The technique gives a meager calculation procedure, yet it retains the comprehensive chemistry of the multi-phase system.

3.2 Heat and mass balances in the thermochemical model

The two material streams in the bed and freeboard of the counter-current rotary drum can be assumed to consist of separate isotropic flowing media, which exchange both heat and matter with each other. The mass and heat flows for a single axial element with control volumes for both bed and gas are schematically shown in Figure 2. The main body of each control volume moves with the gas or bed streams, such volume elements being pairwise coupled with diffusion-kind of material transport from bed to gas and vice versa. Both streams can exchange heat with each other and the surrounding kiln. The mass balance is that of an open (continuous) system.

The enthalpy-heat balance is in the core of the thermodynamic calculation and thus briefly outlined below. During the stationary operation, the intensive quantities remain constant in a fixed position of the reactor and accordingly, temperature and pressure are locally constant in the gas and bed streams. External forces and viscous forces are neglected, and for simplicity one may also assume that during the stationary operation, the total gas pressure is considered constant throughout the drum. The combined heat and momentum balance for a continuous,

stationary stream consisting of isotropic material is then received in terms of a continuous thermodynamic system as follows:

$$-\mathrm{div}\,\mathbf{J}_Q = \frac{C_P}{V}\,\mathrm{grad}\,T + \sum_r \sum_i H_i \nu_{ir} b_r + \sum_i c_i(\mathbf{v}_i - \mathbf{v})\,\mathrm{grad}\,H_i \qquad (1)$$

which gives the divergence of the reduced heat flux ($\mathbf{J}_Q$) in terms of the temperature gradient and the enthalpy changes in chemical reactions and phase transformations (Haase 1969). In equation (1) C_P is molar heat capacity, V is volume of the system, $\mathbf{v}$ is the velocity of the local centre of gravity, whereas $\mathbf{v}_i$ is used for average velocity of the species of type i, c_i denoting their (molar) concentration. The second term on the right hand side gives the change in enthalpy due to chemical reactions or phase transformations, H_i being the molar enthalpy of species i and ν_{ir} the stoichiometric coefficient of species i in reaction r and b_r the reaction or phase transformation rate. The third term includes the enthalpy change due to diffusion of the components (i) of the stream. Supposing that no diffusion does not occur but in the radial direction and this factor then indicates the material exchange between bed and gas (or vice versa, cf. figure 2).

The temperature gradient can further be represented in terms of enthalpies by using the thermodynamic relation

$$\frac{C_P}{V}\,\mathrm{grad}\,T = \sum_i c_i\,\mathrm{grad}\,H_i - \left[1 - \frac{T}{V}\left(\frac{\partial V}{\partial T}\right)_{P,n_i}\right]\mathrm{grad}\,P \qquad (2)$$

Assuming constant pressure and rearranging, the steady state balance applicable for both bed and gas streams becomes

$$\sum_i c_i \left(\mathbf{v}_i - \mathbf{v}\right)\mathrm{grad}\, H_i = -\mathrm{div}\, \mathbf{J}_Q - \sum_r \sum_i H_i \nu_{ir} b_r - \sum_i c_i \mathbf{v}\, \mathrm{grad}\, H_i \qquad (3)$$

The enthalpy transport due to mass interchange between bed and gas (for each control volume) $\sum_i c_i \left(\mathbf{v}_i - \mathbf{v}\right)$ is balanced by heat flux between the control volume element and its surroundings and the enthalpy change in the volume element. The enthalpy change includes the enthalpies of reactions within the control volume and the change of molar enthalpies of the contents in the control volume, as deduced from the respective change of temperature by equation (2).

Alternatively, regarding the control volume element simply an open system operating in the stationary state, there must be $\mathrm{d}H = \mathrm{d}Q$ for each element. Taking into account the temperature change in each volume element, the enthalpy change assuming constant pressure is:

$$\mathrm{d}H = C_P\, \mathrm{d}T + \sum_i H_i\, \mathrm{d}n_i \qquad (4)$$

where $\mathrm{d}n_i = \mathrm{d}_r n_i + \mathrm{d}_e n_i$ with the subscript r referring to changing molar amounts (n_i) due to internal causes (chemical reactions inside the region) and subscript e referring to external causes (mass exchange with the surroundings). The stationary state condition $\mathrm{d}H = \mathrm{d}Q$ leads to:

$$\sum_i H_i\, \mathrm{d}_e n_i = \mathrm{d}Q - \sum_i H_i\, \mathrm{d}_r n_i - C_P\, \mathrm{d}T \qquad (5)$$

Where the left hand side again includes the enthalpy transported by mass exchange with surroundings and the right hand side is given in terms of heat increment and the enthalpy change due to internal causes within the volume element. The respective equations for the 1-

dimensional enthalpy and mass balances of both bed and gas streams are given in detail in the Appendix.

Written in either way, the enthalpy balance is then comparable with e.g. the formalism of Manitius & al. where the enthalpy content of the stream, defined as the product of the mass flow rate of the components and their heat capacities is changing due to enthalpies of reactions and phase transformations and heat transferred between gas and solids and between the furnace walls and the gaseous and solid streams. Thus the formulation of the heat balance in terms of the thermodynamic state quantities gives a compatible treatment with the conventional differential heat balance.

3.3 Gibbs energy model for the kiln chemistry

Gibbs energy of the system in terms of the molar amounts of the constituents and their chemical potentials is given as:

$$G = \sum_{i}^{N} n_i \mu_i = \sum_{i}^{N} n_i \left(\mu_i^{\circ} - RT \ln a_i \right) \qquad (6)$$

The summation covers all species and phases. The detailed mathematical form for the chemical potentials (μ_i) will depend on the applied phase models. While the standard state data for μ_i° is given as program input, the formulas of activities (a_i) often become complex functions of temperature and the amounts of matter. For many rotary kilns it is sufficient for both the bed and the gas to assume that the thermochemical system consists of condensed pure substances and of an ideal gas phase. However, for some applications, such as the lime and cement kiln and some metallurgical furnaces, condensed mixture phases like molten salts and oxide melts also appear, and the thermochemical system must be described as a non-ideal multi-phase mixture, accordingly.

The composition of the multicomponent system is solved by minimising the Gibbs energy as function of the molar amounts (n_i) . The necessary constraints for the minimisation denote the balance equations set on the components forming the constituents of the system. The constraints typically refer to elemental amounts of a closed thermodynamic system, but can also include conservation of various attributes, including the extent of kinetically slow reactions (Pajarre & al. 2016). Using matrix notation, these limitations are expressed as follows:

$$\mathbf{C}^{\mathrm{T}}\,\boldsymbol{n}=\boldsymbol{b} \qquad (7)$$

Here **C** is the conservation matrix, ***n*** the molar amount vector for the constituents and ***b*** is the vector for the amount of the components (in moles) of the Gibbs'ian system

Together, equations (6) and (7) constitute the Gibbs'ian problem to be solved:

$$min\, G(\boldsymbol{n}) \;\text{ s.t. }\; \mathbf{C}^{\mathrm{T}}\,\boldsymbol{n}=\boldsymbol{b} \;\;;\; n_i \geq 0 \;\; \forall\, i \qquad (8)$$

The minimization of Gibbs energy will then be performed in terms of the molar amounts of the constituents of the system with the mass balances (7) as the necessary constraints for the optimisation problem by using conventional min(*G*) subroutines such as ChemApp (Eriksson 1997).

The constraining of slow (non-equilibrium) reactions by their reaction rate data can be realised either by using rate controlled Gibbs energy minimisation (Janbozorgi & al 2009, Elbahloul & al. 2015, Pajarre & al 2016) or by using partitioning of the volume element contents to reactive and non-reactive subsystems. In KilnSimu the latter, computationally less obsessing technique is generally used. In rotary kilns, the bed material consists of particles that typically appear in a non-equilibrium meta-stable state. Most reactions in the bed are gas-solid or solid-solid reactions the kinetics of which are constrained by diffusion

and mass transfer in the bed and inside the particles. The composition of the bed flow in a control volume is calculated by combining the equilibrium with time-dependent particle kinetics. A simple technique is then applied by dividing the condensed phases in the bed into reactive and inert subsystems by calculating the reaction rates of the phase conversions with a first order pseudo-Arrhenius approach used e.g. by Romero-Valle & al (2013) (see equations A7-A10 in the Appendix).

The algorithm of figure 3 provides a stepwise calculation of sequential minima of the Gibbs energy in the bed under the given mass and heat transfer conditions. The iterative procedure in the inner heat transfer algorithm allows for the calculation of temperature as the target variable. In the outer loop, the advancements of selected (slow) chemical reactions are used as additional constraints. Using this procedure for the steadily operating reactor the extensive thermodynamic properties for each positioned element become timely constant and, respectively, the intensive properties at each fixed position also remain unchanged with time. When moving the position of the calculation cells along the longitudinal axis of the kiln, the heat transfer between the system and the surroundings continues and the phase composition of the system changes with the changing temperature. The gaseous species possibly evolved in the bed control volume are removed to the respective gas element. Side streams and effluents can be taken into account as sequential inputs or outputs. With these criteria a series of intermediate steady states is received with known numerical values of their thermochemical properties.

The essential feature of the thermochemical calculation technique is the calculation of the thermodynamic state quantities (both intensive and extensive) for the volume elements of the system. Thus, the same calculation produces in addition to temperatures and molar amounts of substances as well their molar enthalpies, entropies and Gibbs energies. The molar enthalpies, for example, are then used for the aforementioned heat balance calculations.

3.4 Movement of the material bed

The axial velocity of the bed is proportional to inner diameter, rotational speed and inclination of the kiln and is inversely proportional to angle of repose of bed. In addition the bed velocity is inversely proportional to the holdup of the kiln. If considered independent on the holdup (valid simplification for long industrial kiln), then generally the velocity for the axial movement can be given as:

$$v_b = K \frac{d_i \omega f(\psi)}{f(\alpha)} \tag{9}$$

where $f(\psi)$ and $f(\alpha)$ are functions of inclination angle of kiln and angle of repose of bed. The rotational movement of the bed depends on the holdup of the kiln, its angular velocity and the properties of the bed like its porosity, density and viscosity. Material that consists of dry particles behaves very differently than material that contains liquid phases like free water (at lower temperatures) or partly molten slag (formed at higher temperatures). In figure A1 (Appendix) the cross section of the bed is schematically shown. When the angular velocity of the drum is low the bed behaves as a solid object, which proceeds in axial direction as the kiln rotates. The solid particles remain at rest with respect to each other. In practice, the bed will be also sliding with the drum rotation, slumping and rolling. Such phenomena appear to be most important from the point of view of e.g. product particle size and granulation effects, while they are less significant to bed chemistry. Thus, for simplicity, they have not been included in the calculation.

3.5 Boundary values and the solution procedure

As the model structure mimics the physical structure of the actual kilns, the respective parameters must be given in terms of the physical structure of the rotating furnace. This then includes altogether over 20 parameter values, which are derived from the drum geometry, physical properties of the construction materials including furnace linings and the operational data describing the kiln to be simulated. They must describe the length, diameter and optional barriers, chokes (or data of other mechanical devices within the kiln) as well as characterization and geometrical dimensions of the insulating layers. The heat conductivity of the bed usually must be estimated in the program input. While the thermochemical solution applies an algebraic procedure (Eriksson et. al. 1997) and the necessary boundary values thus include only the initial temperatures and mass flows (amounts) of the feed and the ambient temperature of the kiln surroundings. The actual values of the key operational parameters are also part of the input data as shown in Table 1.

Table 1 Input data

Incoming feeds	Mass flows	[ ] kg/h
	Composition	[ ] e.g. mass fractions
	Temperatures	[ ] C {K; F;…}
	Pressures	[ ] bar {atm; kPa; psi; …}
The geometry of kiln	Diameter	[ ] m
	Length	[ ] m
	Number of refractory layers	
	Conductivities of refractories	$W\ m^{-1}K^{-1}$
	Thicknesses of refractory layers	m
Kiln parameters (as input)	Rotational velocity	[ ] $r{\cdot}min^{-1}$
	Inclination	%
	Heat loss in combustion chamber	[ ] kW
	Amount/fraction of recycle gas	[ ] $Nm^{3}{\cdot}\ h^{-1}$
	Leakage air flows	[ ] $Nm^{3}{\cdot}\ h^{-1}$
Bed properties	Angle of repose	deg
	Density	$kg{\cdot}m^{-3}$
	Conductivity	$W\ m^{-1}K^{-1}$
Ambient	Temperature	[ ] C {K; F;…}

The simulation divides the kiln into two compartment fractions: 'bed side' with bed condensed phases, inner and outer wall regions and 'gas side' consisting of freeboard gas regions. First the initial temperature and composition profiles are estimated for the gas flow. After that the temperatures and compositions of all incoming flows to the bed side in the first control volume are known, including the radial mass transfer from the gas side. Then the bed side temperatures are solved from equations (A.3), (A.5) and (A.6) by using appropriate solver (quasi-Newton method) for non-linear set of equations. Each time the solver changes the bed temperature, the equations (A.7) and (A.8) are applied to obtain the bed flow composition and enthalpy. Here, the Gibbs energy minimization for the multiphase system is usually done by calling the ChemApp program library (Eriksson & al. 1997) as a subroutine. After solving the temperatures for the bed side in the first control volume all the flows to the bed side in the second control volume are known. Bed side temperatures and compositions in the second and in all the subsequent control volumes are solved in a similar manner. After that the gas side is calculated by using the previously calculated values for the bed side, including the radial mass transfer from the bed side. Gas flow temperature can be solved from equation (A.4) by using appropriate root-finding solver. Again each time the solver changes the gas temperature the gas flow composition and enthalpy are calculated. After solving both the bed and the gas side, the procedure is repeated until the temperatures in control volumes converge to their final values, which usually takes 10–20 iterations.

The key element affecting the kiln efficiency is the fuel burner, which appears either attached in a separate chamber in front of the kiln or positioned axially inside the rotating kiln jacket. The thermochemical model has an integrated burner calculation allowing for the simulation of optional use of several gaseous, liquid and solid fuels, such as LNG, propane, fuel oils, biomass and various forms of coal under the condition that reliable thermodynamic Gibbs

Energy data is available for these materials. The temperature profiles (or quality factors connected to e.g. bed composition) can then be optimized in terms of the input flows and fuel composition.

The thermodynamic model provides a large variety of numerical data for the user; for example, volumes of flow, enthalpies, heat capacities and heat fluxes, local temperatures and concentrations. From these, the local flow rates for the gas and bed, other properties of the gas and bed and the holdup profile of the furnace can further be calculated. In Table 2, the model results are briefly described.

Table 2. Modelling results

Property	***Description***
The outer wall temperature	The temperature of the outer wall is determined from the convective heat transfer to the ambient air. The temperature profile of the outer wall can be compared directly with measured values and can be used as a control variable for the furnace.
The inner wall temperature	The temperature of the outer wall is determined from the heat transfer from inside the furnace to its outer wall. The temperature profile of the inner wall is an important design parameter for furnace materials.
The gas temperature	The gas temperature is a direct output of the thermodynamic furnace model. It determines the local reaction rates, the local composition and the flow rate of the gas. Inlet and outcoming temperatures can be used to control the kiln operation as well as check points of the model validation.
The bed temperature	The bed temperature results from the thermodynamic model of the bed. It determines the location of phase transition and reaction zones in the solid mass. The bed temperature is a major factor controlling product qualities ant the output temperature of the bed is usually followed as a key operational factor.
Heat fluxes	Heat flows through different parts of the furnace give valuable information of the furnace operation and also for the design of the furnace. For example, the effect of alternative furnace geometries or brick materials can be tested by changing the parameters accordingly in the model.
Heats of reaction	The thermodynamic model provides the heats of reaction and phase transition in various parts of the furnace. The most vigorous reaction zones can thus be located.
Composition of gas	The model provides the user with the dull composition of the gas along the kilns axis. This gives the characteristics of the burner offgas as well as the gaseous products in different zones of the kiln, including the possible emissions of minor volatile species.
Composition of bed	The composition of the bed includes various condensed phases at give point of kiln axis. The bed composition, as well as its temperature, is usually the

	dominant factor on product quality.
Flow rate of gas	The flow rate of the gas is an important scale-up factor for the furnace design. It is affected by burner operations and fuel alternatives as well as by air leakages and gas recycle.
Residence time	The flow rate of the bed gives the total residence time in the kiln. This can be controlled with the furnace tilting angle as well as with its rotation speed.
Holdup	The model provides the user with a 1-dimensional holdup profile of the kiln, defined as the ratio of the cross sectional area of the bed to the cross sectional area of the furnace. The holdup is an important scale-up and runnability factor.

4. Results from cement kiln simulation

4.1 Premises for cement kiln modeling

In this work, the KilnSimu steady state model was applied to a real problem occurring during cement production. The goal was to investigate the impact of an oxygen enrichment at the main burner on the process conditions (temperature profile in the kiln, specific heat consumption) and on the final product quality (clinker mineralogy, free lime) in one of LafargeHolcim's cement plants.

In order to test the model, a reference simulation was performed and compared to available data from a kiln audit in the plant. This reference simulation has the purpose to adjust the kinetic parameters (lime calcination, C_2S formation, C_3S conversion reaction) to match the observed data in the kiln audit.

A full kiln audit is resource and time consuming because steady state conditions are needed to perform a full mass and heat balance. Typical results of kiln audits are raw mix (kiln feed) composition and temperature, clinker compositions and temperature, hot meal composition (calcination degree, mineralogy) and temperature at the kiln entrance, oxygen partial pressures at various locations, total gas flow, dust flow from the preheater tower …

In the case presented here, the results of the kiln audit are average values from three days of continuous measurements.

The key components for the plant layout are summed up in Table 3. It corresponds to a typical dry process with a preheater tower without calciner. The main characteristics of the raw mix and the resulting clinker are presented in Table 4. For the simulation, the kiln was divided into 50 axial control volumes, which consist of bed, gas, inner and outer wall regions.

Table 3: Key data for the cement plant used in this study

Preheater tower	4 stages with 4 cyclones
Rotary kiln	Length 78m, diameter 4.6m, inclination 2.7°, rotation speed 1.7 rpm
Cooler	Grate cooler with 7 fans
Gas flow	121473 Nm^3/h at the stack
Raw mix flow	120 t/h

Table 4: Key chemical data for raw mix and clinker. The modules are calculated from XRF data, the clinker mineralogy was determined by XRD Rietveld analysis

Raw mix	LSF = 96, SM =3.0 , AF = 2.3 , C3S = 67
Clinker	LSF =99, SM =3.1 , AF =2.3 , C3S = 72.5 Mineralogical composition calculated from XRD with the Rietveld method: Alite (C_3S) = 72.5%, Belite (C_2S) = 7.5%, Total Aluminate (C_3A) = 9.5%, Ferrite

	(C_4AF) = 6.5%, Free lime = 0.4%

4.1.1 Thermodynamic database

A key component for the reliability and the quality of the final simulation results is the thermodynamic database used. Various commercial databases are available for oxide systems – FactSage (Bale et al. 2009) , ThermoCalc (Andersson et al. 2002) and MTData (Davies et al 2002) - but all of them are not precise enough to simulate all relevant features of the cement clinkering reactions. The Gibbs energy data for the compounds and phases are often optimized in the silica rich parts of the underlying phase diagrams due to a large variety of available experimental data from the glass manufacturing industry, but the lime rich part is often over-simplified. As an example, the main cement clinker phase, Alite (= Ca_3SiO_5 with dissolved minor elements such as MgO, Al_2O_3, Fe_2O_3) is systematically described as a stoichiometric line compound and not as a solution phase. The solubility of these minor elements were neglected because they are generally below 2 mass%. However, their impact on the final reactivity in the resulting cement is not negligible. Therefore, it was decided to review the existing data to produce a more realistic Gibbs energy dataset for the simulations.

The chemical system used for the simulation is the CaO, SiO_2, Al_2O_3, Fe_2O_3, MgO, Na_2O, K_2O + CO_2, H_2O, O_2, N_2 system. The starting point was the commercial FTOxid and FactPS databases, as included in the FactSage software package (Bale et al 2009). The quality of the database was checked against available key experimental information (Taylor, 1997). As a result, it appeared that the data for Ca_3SiO_5 and Ca_2SiO_4 did not allow to reproduce the known equilibria and associated heats of reaction and therefore the Gibbs energies were modified to match the available experimental information (Ayed et al 1994).

In a second step, the thermodynamic descriptions of the main cement clinker phases were transformed from pure stoichiometric compounds to solution phases by adding the relevant minor elements into the phase descriptions. They were modelled as regular solutions between the pure, stable silicates or aluminates and the corresponding end members with the minor elements. For example, C_3S is described as a regular solution (i.e. with a constant interaction parameter) of Ca_3SiO_5 and Mg_3SiO_5, $Ca_6Al_2O_9$ and $Ca_6Fe_2O_9$. Only the interaction parameters of between the main compound and the end members are adjusted, the ones between the end members only were set to 0 (ideal mixing). The full model descriptions for all relevant phases are presented in Table 5. All relevant model parameters were adjusted by trial and error to match the experimental information (Taylor, 1997).

Table 5: Phase description for the main clinker phases taking into account all minor elements

Phase	ID	Thermodynamic model description
Alite	C_3S	Ca_3SiO_5 with "Mg_3SiO_5", "$Ca_6Al_2O_9$" and "$Ca_5Fe_2O_9$"
Belite	C_2S	Ca_2SiO_4 (γ,β,α',α) with "Mg_2SiO_4", "$Ca_3Al_2O_6$" and "$Ca_3Fe_2O_6$"
Aluminate	C_3A	$Ca_3Al_2O_6$ with "$Ca_3Fe_2O_6$" and "$Ca_2Si_2O_6$"
Ferrite	C_4AF	$Ca_2(Al,Fe)_2O_5$ with "$CaSi_2O_5$" and "$Ca_2Mg_2O_4$"
Lime	C	CaO with "Al_2O_3"

The thermodynamic descriptions and parameters for all other compounds (limestone, clays, water …) and phases (slag liquid, gas…) were accepted from the commercial database.

4.1.2 Heat and mass balance simulations

A steady state 1D heat and mass balance simulation was performed for the full plant. Two different scenarios were simulated: a reference calculation corresponding to the standard production which is compared to experimental data from a kiln audit and a modified calculation in which the gas atmosphere at the main burner was enriched with pure oxygen.

Input parameters for the simulations

Input parameters correspond mainly to kiln feed characteristics (inlet temperature, chemical and mineralogical composition, flow rates), fuel characteristics (temperature, chemical composition and combustion heat, flow rate, injection location) and air entering the system (temperature, humidity, flow rates and injection locations). The kiln audit enables also to assess false air flows (air entering the system due to depressurization and lack of sealing between the process equipment)

All other input parameters are associated with the design of the plant as summed up in Tables 3 and 4.

Results of the reference simulation

A first set of simulations was performed in order to adjust a number of parameters for which no experimental information was available. This is in particular necessary for the reaction kinetics. Lime calcination, C_2S formation and C_3S conversion from CaO and C_2S are known to be kinetically driven. The parameters for the kinetic descriptions were again adjusted by trial and error to fit the mineralogical compositions measured at the kiln inlet (calcination degree + amount of C_2S) and at the cooler outlet (mineralogical composition of the full clinker + amount of unreacted free lime). Another parameter which had to be adjusted was the fuel. In order to simplify the system, pure graphite and hydrogen gas was used for the simulation. In order to be in phase with the experimental data, additional gas and solid ashes were introduced for correction and the amount of graphite and hydrogen was adjusted to fit

the observed combustion heat. It is clear that this presents a simplification. However, the error introduced should be small. The kinetic parameters for the combustion were chosen to get a flame length in agreement with common knowledge.

The result of the reference simulation as compared to the kiln audit parameters is presented in Table 6. The overall agreement is good except for the preheater exhaust temperature and the exhaust oxygen content. The simulated preheater exhaust temperature is ~60K lower than the observed one. The origin of this is unknown. The simulated oxygen partial pressure is lower than the observed one. As for the specific heat consumption, the simulation value agrees with less than 2% difference with the experimental one.

Table 6: Comparison of the main parameters of the kiln audit with the results from the KilnSimu reference simulation

	Kiln audit	KilnSimu reference simulation
Secondary air [Nm3/ kg ck]	1.17	1.07
Exhaust cooler [Nm3/ kg ck]	1.02	1.02
Cooler air [Nm3/kg ck]	2.04	2.09
Preheater exhaust [Nm3/kg ck]	1.70	1.81
Preheat exhaust O_2 [%vol]	6.80	5.85
Preheater temperature [°C]	385	321
Clinker composition		
C_3S	72.5	73.2
C_2S	7.5	10.9
C_3A	9.5	8.2
C_4AF	6.5	6.4
Free lime	0.4	0.2
Specific heat consumption [MJ/kg ck]	3.80	3.86

The influence of oxygen enrichment at the main burner was investigated in a second simulation. The addition of oxygen to the main burner is known to optimize the overall combustion behaviour and therefore to reduce the fuel consumption. However, it is not easy to predict this behaviour quantitatively.

All simulation parameters (kinetic parameters, kiln feed…) were kept identical to the reference calculation. The simulations were performed in such a way that the oxygen partial pressure at the preheater exit as well as the maximum clinker burning temperature were maintained identical to the reference calculation for comparison. To achieve this behaviour, the cooler characteristics had to be changed manually. The gas distribution between the secondary air (going to the kiln outlet) and the exhaust (going to the stack) had to be adjusted manually until agreement was reached between the reference calculation and the oxygen enriched one. Because the simulation is always performed at constant pressure (here: atmospheric pressure), the gas distribution and the neutral point in the cooler is controlled by the cooler stack position. In KilnSimu, the position is numbered from 0 (beginning of the cooler, close to the kiln) to 1 (end of the cooler, clinker outlet). The numerical results of the simulation are presented in Table 7.

The simulated specific heat consumption has effectively been reduced by approximately 1% with very low impact on the bed temperature profile (Figure 4) and on clinker quality (Figure 5).

Table 7: comparison in between normal burning conditions and with an oxygen enriched air at the main burner

	Reference simulation	30% O_2 at main burner

	simulation	burner
Stack position	0.83	0.78
Oxygen concentration preheater exit [%vol]	6.48	6.43
Maximum clinker temperature [°C]	1420	1415
Calcination rate at kiln inlet [%]	23	20
Specific heat consumtion [MJ/kg ck]	3864	3863
Preheater temperature [°C]	321	310
Gas flow at preheater exit [Nm3/kg ck]	1.81	1.74
Specific heat consumption [MJ/kg ck]	3.80	3.86

5. Conclusion

The increased industrial effort towards more resource efficient processes and recycling of material values are further augmenting the employment of rotary kilns as one of the best available methods in processing of both primary and recycled materials. Even though the kilns represent Best Available Technology in many of their applications, there is substantial potential in improving their material and energy efficiency by using computational process chemistry. The combined thermochemical and kinetic algorithm used in KilnSimu provide efficient and accurate steady state simulation of rotary furnaces by utilizing available thermodynamic and kinetic data. The model could be successfully applied to an industrial cement clinkering case. The agreement of the simulation with observed experimental data is good. The impact of oxygen enrichment at the main burner was simulated and a reduction of specific heat consumption was predicted.

6. References

1. Andersson, J.-O., Helander, T., Höglund, L., Shi, P., Sundman, P. : ThermoCalc & Dictra, computational tools for materials science, Calphad 26(2) (2002) 273-312
2. Ayed, F., Sorrentino, F., Castanet, R.: Determination par calorimetrie de dissolution des enthalpies de formation de quelques silicates, aluminates et alumino-silicates de calcium, Journal of Thermal Analysis & Calorimetry 41(4) (1994) 755-766 [doi: 10.1007/BF02547157]
3. Backman, R., Hupa, M. and Tran, H.: Modelling the sodium enrichment in lime kilns, Pulp & Paper Canada, 1993, 94:11, T387-T391.
4. Bale, C.W., Bélisle, E., Chartrand, P., Decterov, S.A., Eriksson, G., Hack, K., Jung, I.-H., Kang, Y.-B., Melançon, J., Pelton, A.D., Robelin, C., Petersen, S.: Factsage thermochemical software & databases – recent developments, Calphad 33(2) (2009) 295-311
5. Barr, P. V. , Brimacombe, J. K., Watkinson, A. P.: A heat-transfer model for the rotary kiln: Part I. pilot kiln trials, Metallurgical Transactions B, June 1989, Volume 20, Issue 3, pp 391-402[DOI: 10.1007/BF02696991]
6. Barry, T.I., Glasser, F.P. : Calculations of Portland cement clinkering reactions, Adv. Cement Res. 12(1) (2000) 19-28
7. Boateng, A.A., Barr, P.V.: A thermal model fort the rotary kiln including heat transfer within the bed, Int. J. Heat Mass transfer 1996, 39, No 10, 2131-2147[http://dx.doi.org/10.1016/0017-9310(95)00272-3]
8. Boateng, A.A.: Rotary Kilns: Transport Phenomena and Transport Processes, Elsevier, 2008.

9. Davies, R.H., Dinsdale, A.T., Gisby, J.A., Robinson, J.A.J., Martin, S.M.: MTDATA – thermodynamic and phase equilibrium software from the National Physical Laboratory, Calphad 26(2) (2002) 229-271

10. Dumont, G., Belanger, P.R.: Steady State Study of a Titanium Dioxide Rotary Kiln, Ind.Eng.Chem. Process Des.Dev., **17**, No2, 107-114, (1978).[DOI: 10.1021/i260066a001]

11. Elbahloul, S. Rigopoulos, S. (2015): Rate-Controlled Constrained Equilibrium (RCCE) simulations of turbulent partially premixed flames (Sandia D/E/F) and comparison with detailed chemistry, Combustion and Flame 162, 2256–2271, http://dx.doi.org/10.1016/j.combustflame.2015.01.023

12. Eriksson, G. , Hack, K. and Petersen, S.: Werkstoffswoche '96, Symposium 8: Simulation Modellierung, Informationsysteme, 1997, 47, ISBN3-88355-236-4, DGM Informationsgesellschaft, mbH, Frankfurt, Germany.

13. Eriksson, M. (Nordkalk Oy, Finland), Karema, H., Boström, S. (Process Flow Oy, Finland), Koukkari, P. and Penttilä, K. (VTT, Finland): Coupled Fluent-KilnSimu Simulation of a Rotary Lime Kiln, IFRF TOTeM 33 - Challenges in Rotary Kiln Combustion Processes, Pisa Italy, 11th-12th February, 2009.

14. Eriksson, M., Hökfors, B. and Backman, R.: Oxyfuel combustion in rotary kiln lime production, Energy Science & Engineering (2014), 2 (4), 204-215.[DOI: 10.1002/ese3.40]

15. Ginsberg, T. and Modigell, M.: Dynamic modelling of a rotary kilns for calcination of titanium dioxide white pigment, Computers and Chemical Engineering (doi:10.1016/j.compchemeng.2011.03.029)

16. Ginsberg, T., Liebig, D., Modigell, M., Hack, K. and Yousif, S.: Simulation of a cement plant using thermochemical and flow simulation tools, in (Puigjaner, L. and

Espuna A., editors): European Symposium on Computer Aided Process Engineering 15; Elsevier Science B.V. 2005

17. Haase, R.: Thermodynamics of Irreversible Processes, Dover Publications Inc. New York, 1969
18. Janbozorgi, M., Ugarte, S., Metghalchi, H., & Keck, J.C. (2009). Combustion modeling of mono-carbon fuels using the rate-controlled constrained-equilibrium method. Combust. Flame, 156, 1871-1885.[doi:10.1016/j.combustflame.2009.05.013]
19. Ketonen M., Koukkari P. and Penttilä K.: Simulation Studies of the Calcination Kiln Process, The European Control Conference, ECC 97, Brussels, Belgium 1-4 July, 1997.
20. Koukkari, P., Laukkanen, I., Liukkonen, S.: Combination of overall reaction rate with Gibbs energy minimization, Fluid Phase Equilibria, (1997) No: 136, 345 - 362 . [doi:10.1016/S0378-3812(97)00123-4]
21. Koukkari, P.: A Physico-Chemical Method to Calculate Time-Dependent Reaction Mixtures, Computers & Chemical Engineering, Vol. 17, (1993) No. 12, pp. 1157 – 1165.[doi:10.1016/0098-1354(93)80096-6]
22. Koukkari, P.: A Physico-chemical Reactor Calculation by Successive Stationary States, Acta Polytech. Scand., Chemical Technology series 224, The Finnish Academy of Technology, Helsinki, 1995.
23. Koukkari, P.; Pajarre, R.: Introducing Mechanistic Kinetics to the Lagrangian Gibbs Energy Calculation, Computers and Chemical Engineering, Vol 30 (2006), 1189-1196. [http://dx.doi.org/10.1016/j.compchemeng.2006.03.001]
24. Mager, K., Meurer, U., Garcia-Ecocheaga, B., Goigoechea, N., Rutten, J., Saage, W., Simonetti, F.: Recovery of Zinc Oxide from Secondary Raw Materials: New

Developments of the Waelz Process, Recycling of Metals and Engineered Materials, Editors: Stewart, D.L.,Stephens, R. and Daley J.C., TMS (The Minerals, Metals and Materials Society, 2000, 329-344.

25. Manitius,A., Kurcyuz,E., Kawecki,W.: Mathematical Model of the Aluminum Oxide Rotary Kiln, Ind. Eng.Chem. Process Des. Develop., 13, No 2, 132-142, (1974)[DOI: 10.1021/i260050a007]
26. Marias, F., Roustan, H., Pichat,A.: Modelling of a rotary kiln for the pyrolysis of aluminium waste, Chem.Eng.Sci. 60 (2005) 4609 – 4622 [http://dx.doi.org/10.1016/j.ces.2005.03.025]
27. Mastrorakos, E., Massias, A., Tsakiroglou, C.D., Goussis, D.A., Burganos, V.N., Payatakes, A.C.: CFD predictions for cement kilns including flame modelling, heat transfer and clinker chemistry, Applied Mathematical Modelling 23 (1999) 55-76 [http://dx.doi.org/10.1016/S0307-904X(98)10053-7]
28. Modigell, M. and Liebig, A.: Thermochemical Process Modelling of Clinker Burning, GTT Product Presentation and Workshop, Aachen, Germany 6.-8.6. 2002
29. Mujumdar, K.S, Ganesha, K.V., Kulkarni, S. B., Ranade, V. V.: Rotary Cement Kiln Simulator (RoCKS): Integrated modeling of pre-heater, calciner, kiln and clinker cooler, Chemical Engineering Science 62 (2007) 2590 – 2607.[http://dx.doi.org/10.1016/j.ces.2007.01.063]
30. Mujumdar, K.S. and Ranade, V.V.: Simulation of rotary cement kilns using a one-dimensional model, Chemical Engineering Research and Design, 84 (A3), 165-177, (2006)[http://dx.doi.org/10.1205/cherd.04193]
31. Pajarre, R., Koukkari, P. & Kangas, P., 2016. Constrained and extended free energy minimization for modelling of processes and materials, Chem. Eng. Sci. 146, 244-258.

32. Penttilä, K., A Simulation Model of TiO_2-calcination Kiln, M.Sc. thesis, Helsinki University of Technology, Faculty of Process Engineering and Materials Science, 1996.

33. Pisaroni, M, Sadi, R & Lahaye, DJP (2012). Counteracting ring formation in rotary kilns. Journal of Mathematics in Industry, 3(2), 1-19.

34. Romero-Valle, M.A. , Pisaroni, Van Puyveldeb, M.D., Lahayea, D.J.P., Sadic, R. (2013): Numerical Modeling of Rotary Kiln Productivity Increase, Reports of the Department of Applied Mathematics 13-09. Delft: EWI Dept. Applied Mathematics.

35. Stadler, K.S., Poland, J., Gallestey, E.: Model predictive control of a rotary cement kiln, Control Engineering Practice 19 (2011) 1-9 [http://dx.doi.org/10.1016/j.conengprac.2010.08.004]

36. Taylor, H.F.W. : Cement chemistry, 2nd edition, Thomas Telford (1997)

37. http://www.vttresearch.com/services/smart-industry/metals-and-minerals-recovery-and-reuse/design-of-sustainable-materials-and-machinery/modelling-and-simualtion (17.3. 2015)

38. http://gtt.mch.rwth-aachen.de/gtt-web/kilnsimu (1.12. 2014)

39. www.rccm.co.jp (17.3. 2015)

40. http://www.kilnsimu-fks.com/ (1.12. 2014)

41. Yokota, M.: Application of "KilnSimu" for Industrial Scale Rotary Kiln Analysis in UBE Industries, Finnish-Japanese Seminar and ChemSheet Short Course 31.8. -2.9. 2009, Espoo, Finland.

Appendix

Heat and material balances in the 1-dimensional KilnSimu solution

In the operating steady state the mass and energy balances for the bed and the gas flows and energy balances for the inner and the outer wall in control volume *k* are given as:

$$\dot{m}_{bb}^{k-1} + \dot{m}_{gb}^{k} + \dot{m}_{fb}^{k} - \dot{m}_{bb}^{k} - \dot{m}_{bg}^{k} = 0 \quad \textbf{(A.1)}$$

$$\dot{m}_{gg}^{k-1} + \dot{m}_{bg}^{k} + \dot{m}_{fg}^{k} - \dot{m}_{gg}^{k} - \dot{m}_{gb}^{k} = 0 \quad \textbf{(A.2)}$$

$$H_{bb}^{k-1} + H_{fb}^{k} - H_{bb}^{k} + H_{gb}^{k} - H_{bg}^{k} + Q_{gb}^{k} + Q_{ib}^{k} = 0 \quad \textbf{(A.3)}$$

$$H_{gg}^{k-1} + H_{fg}^{k} - H_{gg}^{k} + H_{bg}^{k} - H_{gb}^{k} - Q_{gb}^{k} - Q_{gi}^{k} = 0 \quad \textbf{(A.4)}$$

$$Q_{gi}^{k} - Q_{ib}^{k} - Q_{io}^{k} = 0 \quad \textbf{(A.5)}$$

$$Q_{io}^{k} - Q_{os}^{k} = 0 \quad \textbf{(A.6)}$$

There is incoming axial bed flow from the previous control volume and incoming axial gas flow from the next control volume. There can be one or more feed flows from the surroundings to the bed and the gas regions. Outgoing flows have the same temperatures and the compositions as in their source regions.

There are also radial flows between the bed and the gas regions in the control volume. The flow from the bed consists of evaporated gas and solid dust carried away with gas flow. The flow to the bed is composed of the gas interacting with the bed surface and solid particles returning back to the bed. In the model the gas phase has a mixing coefficient that determines the fraction of gas interacting with the bed. Also each solid phase has a dusting and saltation coefficients that are used to calculate the mass fractions of the phase constituents transported from the bed to the gas $\bar{x}_{bg}^{k}$ and back to the bed $\bar{x}_{gb}^{k}$.

The bed and gas flows in the regions are described as thermodynamic systems, which transform mass and heat with each other and their surroundings. Thermodynamic system consists of gaseous and other mixture phases, and number of stoichiometric condensed phases. The equilibrium state of the system can be determined by minimizing its Gibbs energy at constant temperature and pressure. KilnSimu uses ChemApp programming library to calculate the Gibbs energy minimum as well as the enthalpies and heat capacities of the bed and the gas flows.

Bed material consists of particles that are typically at meta-stable state. Most reactions in the bed are gas/solid or solid/solid reactions that are constrained by diffusion and mass transfer in the bed and inside the particles. The composition of the bed flow in a control volume is calculated by combining the equilibrium with time-dependent particle kinetics. In basic KilnSimu the condensed phases in the bed are divided into reactive and inert subsystems by calculating the reaction rates of the respective phase conversion. The equilibrium calculation is then performed for the mass flows of the reactive phase constituents only:

$$\bar{x}_b^k = \bar{A}_0 \exp\left(-\bar{E}_a / RT_b^k\right)\Delta t^k \qquad \textbf{(A.7)}$$

$$\bar{m}_b^k = \bar{G}_{min}\left(T_b^k, P_b^k, \bar{x}_b^k\left(\bar{m}_{bb}^{k-1} + \bar{m}_{fb}^k + \bar{m}_{gb}^k\right)\right) + \left(1 - \bar{x}_b^k\right)\left(\bar{m}_{bb}^{k-1} + \bar{m}_{fb}^k + \bar{m}_{gb}^k\right) \qquad \textbf{(A.8)}$$

$$\bar{m}_{bg}^k = \bar{x}_{bg}^k \bar{m}_b^k \qquad \textbf{(A.9)}$$

$$\bar{m}_{bb}^k = \left(1 - \bar{x}_{bg}^k\right)\bar{m}_b^k \qquad \textbf{(A.10)}$$

where $\bar{x}_b^k$ are the mass fractions of the constituents in the reactive part of the phase calculated with first order reaction rate equations. The data for such conversions is often not available but adjustment according to observed fractionation in any typical process must be used. For example

for $CaCO_3$ calcination in a cement kiln $\vec{A}_0 = 120\ s^{-1}$ and $\vec{E}_a = 8400\ \mathrm{J} \cdot mol^{-1}$ have been used. The other respective phase transformations include the phases listed in Table 5. More complex particle kinetics, such as the shrinking core model can additionally be used. The composition of the gas stream is calculated following similar principles and e.g. fuel burning kinetics then becomes taken into account.

The heat transfer flows in control volume k are calculated with simple heat conduction equations as follows:

$$Q_{gb}^k = h_{gb}^k A_{gb}^k \left(T_g^k - T_b^k\right) + \overline{GS_b}^k \sigma \left(T_g^{k4} - T_b^{k4}\right) \quad \textbf{(A.11)}$$

$$Q_{gi}^k = h_{gi}^k A_{gi}^k \left(T_g^k - T_i^k\right) + \overline{GS_i}^k \sigma \left(T_g^{k4} - T_i^{k4}\right) \quad \textbf{(A.12)}$$

$$Q_{ib}^k = h_{ib}^k A_{ib}^k \left(T_i^k - T_b^k\right) + \overline{S_i S_b}^k \sigma \left(T_i^{k4} - T_b^{k4}\right) \quad \textbf{(A.13)}$$

$$Q_{io}^k = 2\pi L^k \left(T_i^k - T_o^k\right) \Big/ \sum_l \frac{1}{k_l^k} \ln \frac{d_{l+1}^k}{d_l^k} = 2\pi L^k R^k \left(T_i^k - T_o^k\right) \quad \textbf{(A.14)}$$

$$Q_{os}^k = h_{os}^k A_{os}^k \left(T_o^k - T_s\right) + \overline{S_o S_s}^k \sigma \left(T_o^{k4} - T_s^{k4}\right) \quad \textbf{(A.15)}$$

Forced convective heat transfer takes place between the gas and the inner wall and the bed surface. There are many correlations in the literature that can be used to calculate the heat transfer coefficient as a function of gas flow properties, like its velocity, density, viscosity and thermal conductivity. In addition, KilnSimu also uses temperature dependent equations for gas species to calculate viscosity and thermal conductivity of the gas flow.

Conductive heat transfer takes place between the inner wall and the bed. The penetration theory can be used to derive the conductive heat transfer coefficient between the inner wall and the bed:

$$h_{ib} = \frac{2k_b}{\sqrt{\pi \alpha_b \tau_{ib}}} \quad \textbf{(A.16)}$$

Heat transfer is more efficient the shorter the contact time τ_{ib} between the inner wall and the bed is. Radiation model consists of radial heat exchange between gray gas and reradiating bed and inner wall surfaces, i.e. radiation between the regions in the control volume. Total energy balance can be written over each region in terms of the radiation arriving at it from all other regions in the control volume (axial radiation is neglected). Radiation equations are written in terms of total exchange factors, which are functions of emissivities and geometries of regions. Total exchange areas can be solved from the resulting system of linear, algebraic equations.

The measured emissivity and absorptivity of carbon dioxide and water vapour are tabularized as function of their partial pressures, temperature and mean path length. KilnSimu uses Leckner correlation based on these tables to calculate the emissivity and absorptivity of the gas phase. The emissivity of the soot particles is generally also included.

Nomenclature

A Heat transfer area, () m^2.
$\vec{A}_0$ Vector of frequency factors of phase constituents, () 1/s.
a_i Thermodynamic activity of constituent i.
b_r Reaction or phase transformation rate mol/(m^3·s).
$\boldsymbol{b}$ Vector for the amount of the thermodynamic components b_j () mol.
$\mathbf{C}$ Mass conservation matrix of the thermodynamic system with stoichiometric elements c_{ij}.
C_P Molar heat capacity () J/(mol·K).
c_i Molar concentration of species i mol/m^3.
d Diameter, () m.
Δt Residence time (L/v), () s.
$\vec{E}_a$ Vector of activation energies of phase constituents, () J/mol.
G Gibbs energy, () J/mol.
$\vec{G}_m$ Function that returns vector of mass flows of phase constituents at equilibrium, () kg/s.
$\overline{GS}$ Total exchange area between gas and surface, () m^2.
h^n Heat transfer coefficient, () W/(m^2·K)
H Enthalpy flow, () W.
H_i Molar enthalpy of species i () J/mol.
$\mathbf{J}_Q$ Heat flux () W/m^2.
k Thermal conductivity, () W/(m·K)
K Proportionality constant, () 1/rad.
L Length, () m.
$\vec{m}$ Vector of mass flows of phase constituents, () kg/s.
n Molar flow of phase constituents, () mol/s.
n_i Molar amount of phase constituent (species) i () mol.
$\boldsymbol{n}$ Molar amount vector for the constituents () mol.
P Pressure, () Pa.
Q Heat flow, () W.
R Thermal resistivity, () (m·K)/W.
R Gas constant, () 8.314472 J/(mol·K)
$\overline{SS}$ Total exchange area between two surfaces, () m^2.
T Temperature, () K.
v Velocity, () m/s.
$\mathbf{v}$ Velocity of the local center of gravity () m/s.
$\mathbf{v}_i$ used for average velocity of the species of type i () m/s.
V Volume () m^3.
$\vec{x}$ Vector of mass fractions of phase constituents, ().

Greek symbols

α	Thermal diffusivity ($k/c_p\rho$), () m^2/s.
β	Angle of repose, () rad.
ϕ	Filling angle, () rad.
υ_{ir}	Stoichiometric coefficient of species *i* in reaction *r*
μ_i	Chemical potential of constituent *i* () J/mol.
μ_i°	Chemical potential of constituent *i* in the standard state () J/mol.
σ	Stefan-Bolzmann constant, () $5.67032 \cdot 10^{-8}$ $W/(m^2 \cdot K^4)$.
τ	Contact time (β/ω), () s.
ω	Angular velocity, () rad/s.
ψ	Inclination angle, () rad.
ξ	advancement of a chemical reaction, ( )

Subscripts And Superscripts

b	Bed
f	Feed
g	Gas
i	Inner wall, Index of a chemical constituent (species)
o	Outer wall
p	product
r	reactant
r	index for chemical reaction *r*
s	Surroundings, surface
k	Control volume
l	Wall layer

$\mathrm{d}n_i = \mathrm{d}_r n_i + \mathrm{d}_e n_i$ increment of changing molar amount (n_i) due to internal and external causes (chemical reactions inside the region, subscript *r* ; mass exchange with the surroundings, subscript *e*)

Figure captions

Figure 1: Model scheme of the counter current rotary kiln

Figure 2: KilnSimu mass and heat balance modeling

Figure 3: Iteration algorithm for the rotary kiln balances (r=reactant, p=product, ξ=advancement of reaction)

Figure 4: Clinker bed temperature profile in the kiln and the cooler (with and without oxygen addition)

Figure 5: Clinker and gas composition profiles in the kiln and the cooler (with and without oxygen addition)

Figure A.1: Radial heat flows and bed geometry (left) and axial and radial flows to and from a control volume and temperatures in it

Figures

Figure 1

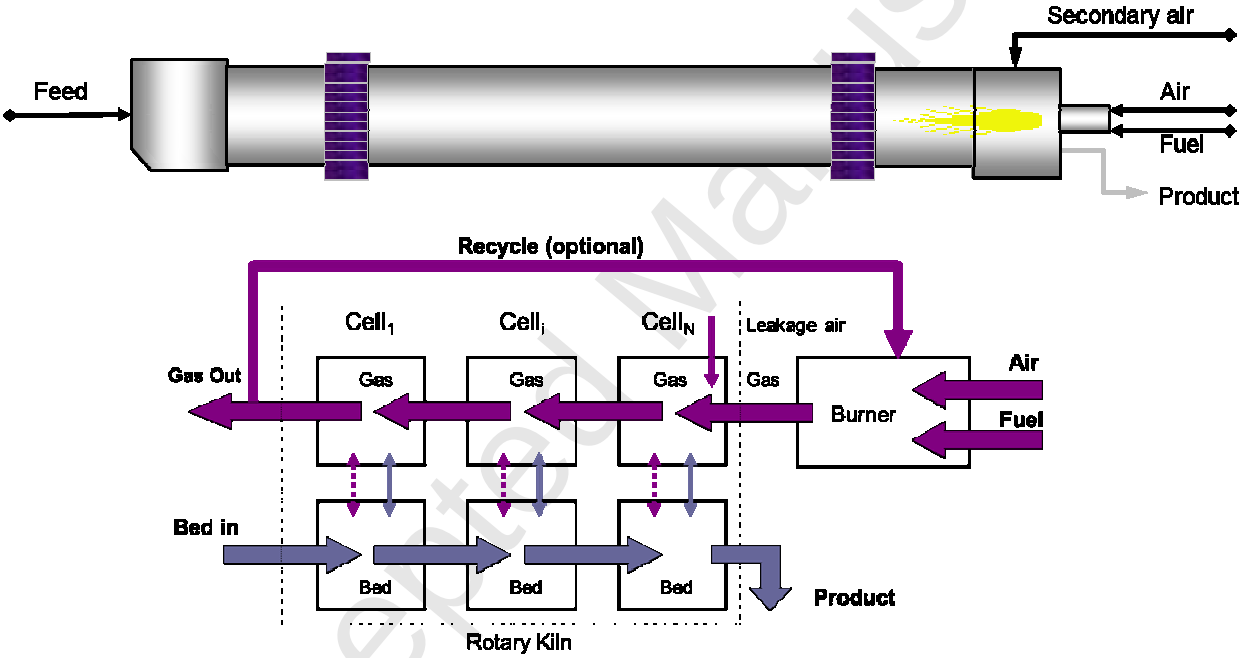

Figure 2

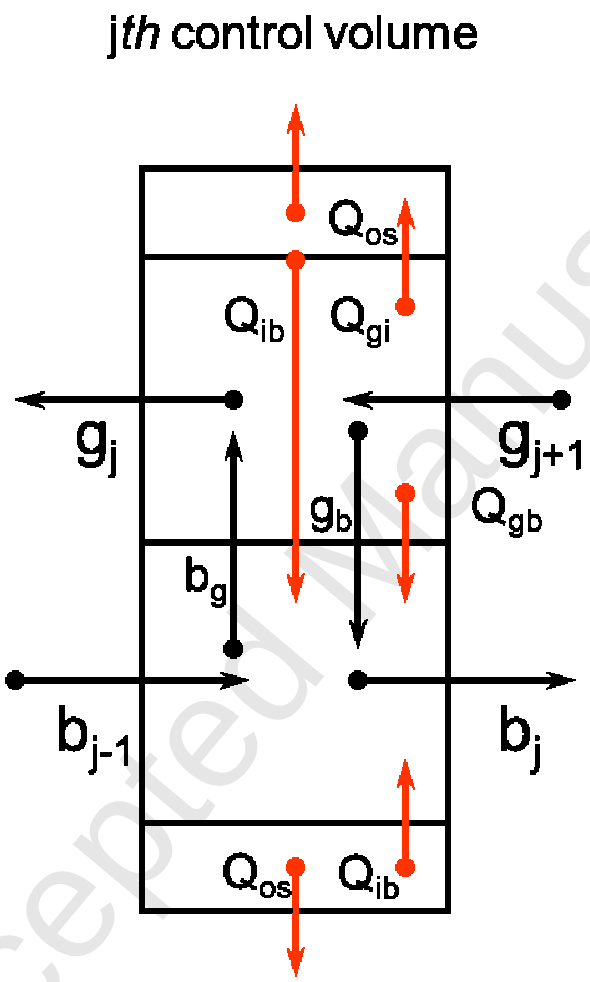

Figure 3

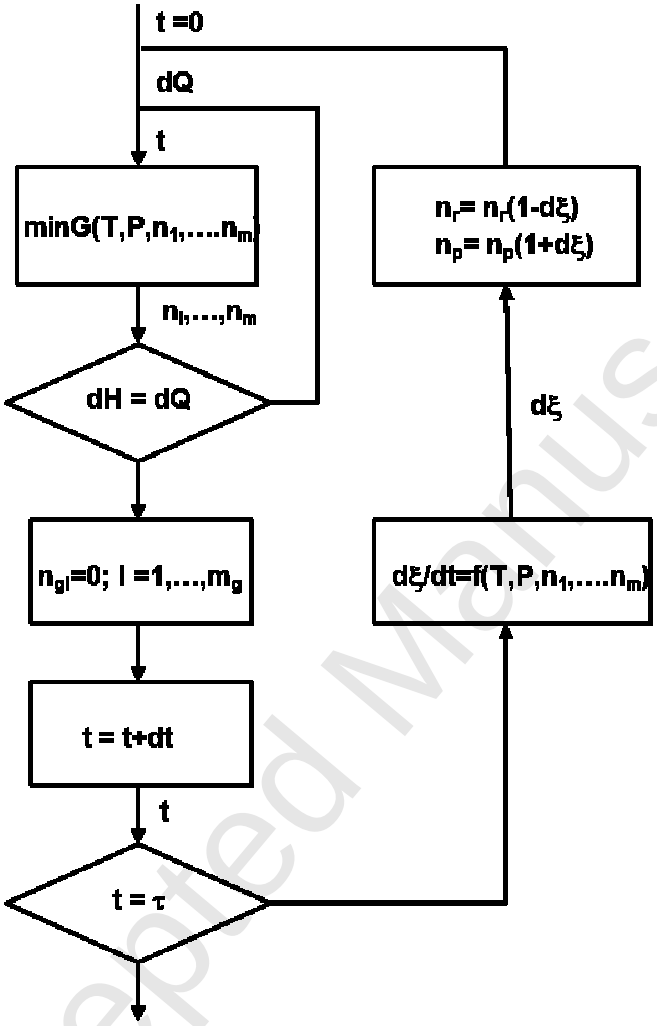

Figure 4

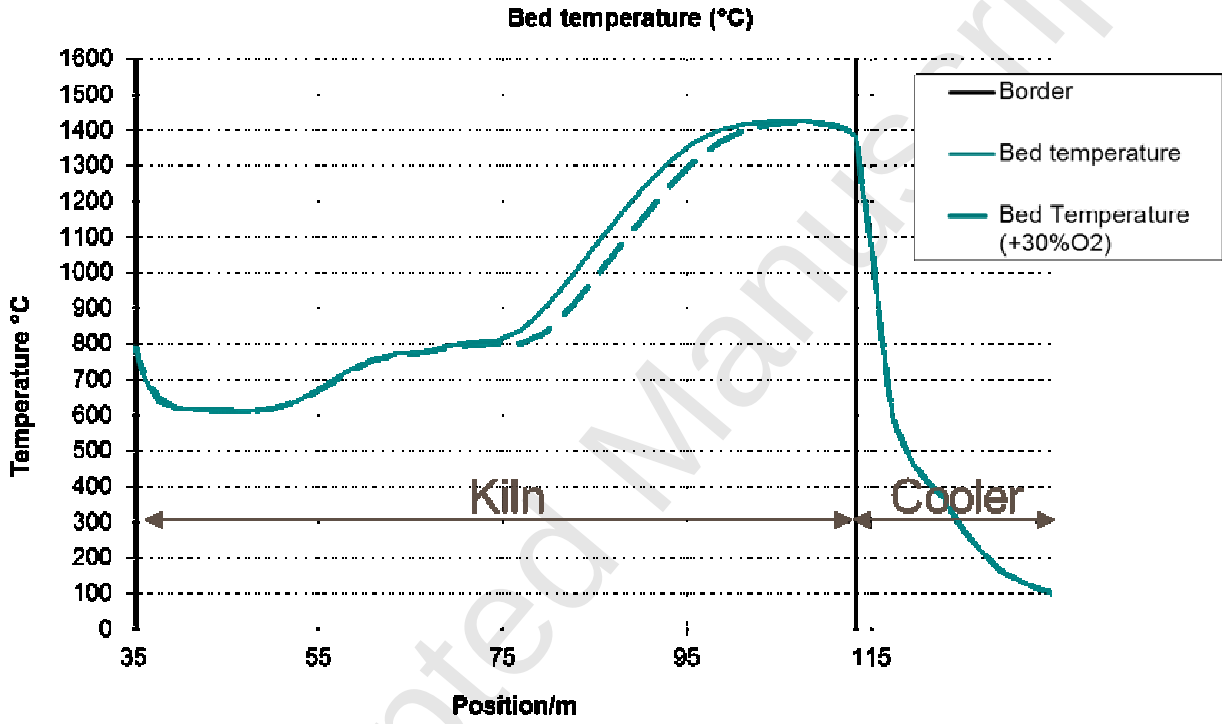

Figure 5

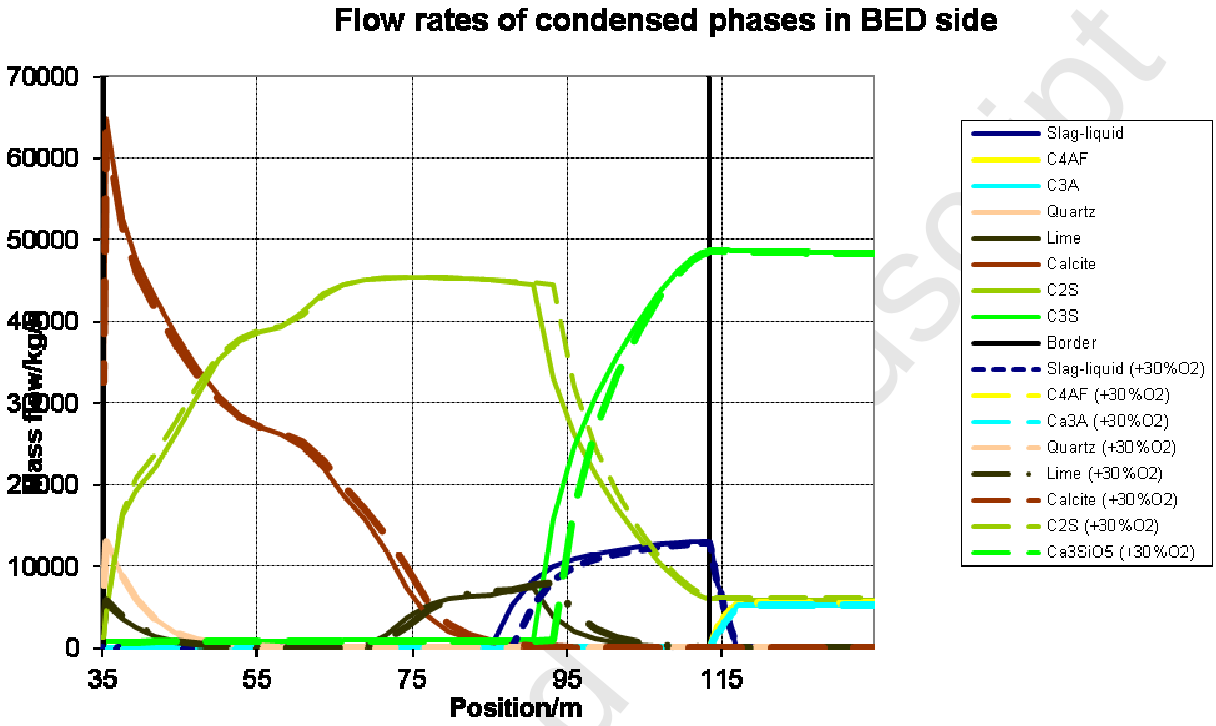

Figure A.1

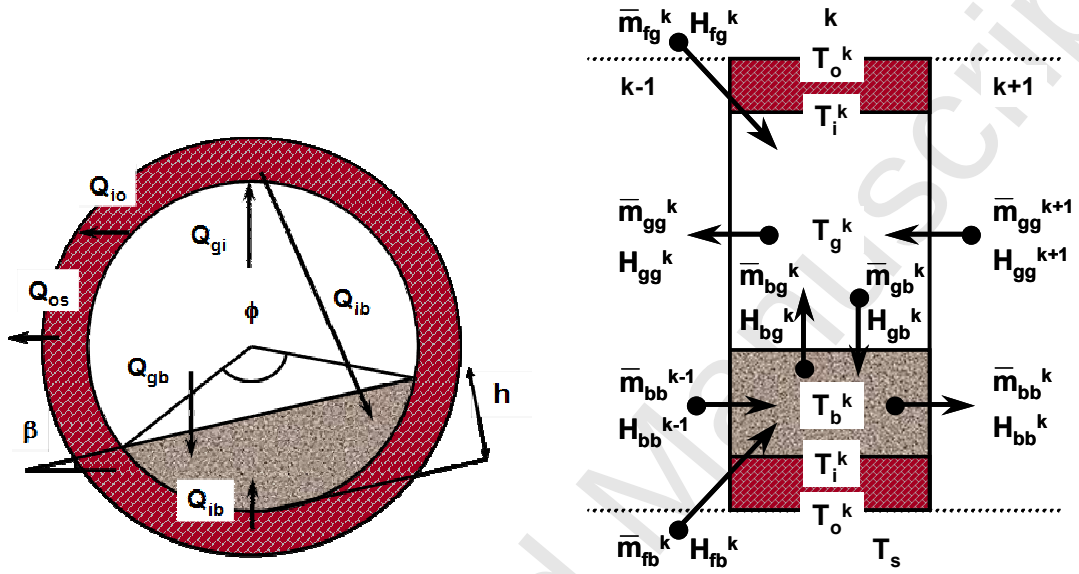

Research highlights:

- Advanced Gibbs Free energy minimization applied for modelling physical and chemical processes in various industrial rotary kilns
- A combined model of thermochemistry and kinetics for rotary kilns
- KilnSimu application to an industrial case in cement clinker manufacturing